

扩散相关光谱组织血流检测及其临床应用

李哲^{1,2,3*}, 冯金超^{1,2,3**}, 贾克斌^{1,2,3***}

¹北京工业大学信息学部, 北京 100124;

²先进信息网络北京实验室, 北京 100124;

³北京工业大学计算智能与智能系统北京市重点实验室, 北京 100124

摘要 扩散相关光谱(DCS)技术是一种新兴的组织血流无创检测技术。该技术将近红外光照射到组织表面,通过计算组织表面散射光斑的光强自相关函数推算组织中红细胞的运动状态,以实现组织血流变化的定量检测。相比于其他血流检测技术,如激光多普勒(LDF)、核磁共振成像(MRI)、正电子发射断层成像技术(PET)等,该技术具有无创、无辐射、可长时间连续实时检测、适用范围广、检测要求低等优势,适宜床边监测。分别从DCS技术的基本原理、系统与方法、临床应用等方面对其进行简要综述,并对DCS技术的未来发展趋势进行展望。

关键词 生物技术; 扩散相关光谱技术; 近红外光谱技术; 组织血流; 心脑血管类疾病; 癌症

中图分类号 R318

文献标志码 A

doi: 10.3788/LOP202259.0617006

Diffusion Correlation Spectroscopy for Tissue Blood Flow Monitoring and Its Clinical Applications

Li Zhe^{1,2,3*}, Feng Jinchao^{1,2,3**}, Jia Kebin^{1,2,3***}

¹Faculty of Information Technology, Beijing University of Technology, Beijing 100124, China;

²Beijing Laboratory of Advanced Information Networks, Beijing 100124, China;

³Beijing Key Laboratory of Computational Intelligence and Intelligent System, Beijing University of Technology, Beijing 100124, China

Abstract Diffusion correlation spectroscopy (DCS) is a relatively new methodology that has been extensively used for the noninvasive monitoring of tissue blood flow. This technology irradiates the tissue surface with near-infrared light, calculates the light intensity autocorrelation function of the scattered spot on the tissue surface, and computes the movement of red blood cells to realize the quantitative detection of blood flow changes in tissues. DCS measurements show more promise for the noninvasive, radiation-free, continuous and real-time monitoring, wide application range, and low detection requirements of tissue blood flow than the other blood flow monitoring methods such as laser Doppler flowmetry (LDF), magnetic resonance imaging (MRI), and positron emission tomography (PET). Moreover, DCS technology can be utilized for the bedside monitoring of tissue blood flow. The DCS technique is mainly introduced in which its theoretical background, instrumentation, progress, and clinical applications are included, as well as its future development prospects are discussed.

Key words biotechnology; diffusion correlation spectroscopy; near-infrared spectroscopy; tissue blood flow; cardiovascular and cerebrovascular disease; cancer

收稿日期: 2021-12-17; 修回日期: 2022-01-13; 录用日期: 2022-01-17

基金项目: 国家自然科学基金(62105010,81871394)

通信作者: *lizhe1023@bjut.edu.cn; **fengjc@bjut.edu.cn; ***kebinj@bjut.edu.cn

1 引言

脑卒中、冠心病、外周动脉疾病等心脑血管类疾病严重威胁着人类生命健康,我国心脑血管类疾病发病率排名世界第一且有年轻化趋势^[1]。对脑组织、骨骼肌组织等血流的长时间、连续、实时无创检测是提升此类疾病治疗效果和避免复发的关键。然而,组织血流作为表征人体生命健康最重要的指标之一,目前的临床技术却无法满长时间、连续、实时无创的床边检测要求。以脑疾病为例,脑血管常规检查一般采用颅脑 CT^[2]、颅脑核磁共振成像(MRI)^[3]或经颅多普勒(TCD)^[4]等方法进行,依据脑血流、脑氧代谢分数等参数综合进行人工诊断^[5-6]。对肾脏功能不全的患者不能使用造影剂进行 CT 血管成像检查,对患有幽闭恐惧症或体内有金属植入物如假牙、心脏支架等患者不能进行颅脑核磁共振检查。上述方法均无法提供长时间连续实时的组织血流无创检测^[7-9]。

扩散相关光谱(DCS)技术是一种利用近红外光进行组织血流无创检测的新兴技术^[10-12]。早在 90 年前,人们就希望通过光来“看见”生物组织中的肿瘤。在 20 世纪 70 年代,650~950 nm 生理窗口被证明在此波段内光子可以在生物组织中穿透得更深,原因在于水和血红蛋白在此波段的吸收较弱^[12]。基于此,近红外光谱技术(DOS 或 NIRS)和扩散断层成像(DOT)得以快速发展,可实现对组织

内含氧血红蛋白和脱氧血红蛋白浓度等参数的测量^[13]。不容忽视的是,生物组织散射光斑的波动对组织内散射体(如红细胞)的运动非常敏感,而对这种多次动态光散射的测量涉及 DCS 技术。DCS 技术既依赖于光场的时间相关也符合扩散方程,因此 DCS 既具有 NIRS/DOS 的光穿透优势,又由于其测量红细胞运动,可实现对组织血流量的检测。DCS 组织血流检测已经通过在体试验被多普勒^[14-15]、核磁共振成像^[16-17]、CT^[18]等多种临床血流检测技术验证,且将 DCS 与 DOS/DOT 相结合^[19-20]可以实现对组织氧代谢等多生理参数的连续实时检测,有助于对脑疾病、骨骼肌疾病和癌症等的初筛、预后和监测,更好地服务于人民关心的重大疾病。

本文分别从 DCS 的基本原理、系统与方法、临床应用等方面综述国内外 DCS 技术的研究现状及进展,并分析该技术的发展趋势。

2 扩散相关光谱技术

2.1 DCS 背景与原理

DCS 技术是在动态光散射(DLS)技术的基础上提出的^[11-12],将近红外光照射到组织表面,通过计算组织表面散射光斑的光强自相关函数 $g_2(\tau)$ 推算组织中红细胞的运动状态,拟合出用于表征组织血流变化的血流指数(BFI),从而实现对组织血流的定量检测,如图 1 所示。

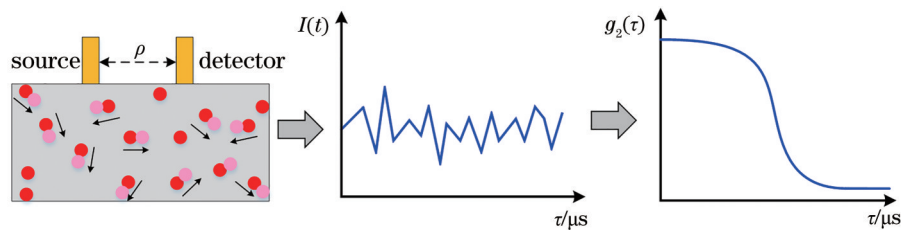


图 1 扩散相关光谱技术原理示意图

Fig. 1 Schematic of diffusion correlation spectroscopy

通常,生物组织被认为是强散射体,存在一些散射体是静态的(或运动异常缓慢的),存在一些散射体是动态的,其中红细胞被认为是主要的动态散射体。对于动态散射体而言,通过多重散射理论可推导出相关传输方程,其可简化为相关扩散方程^[10-11]:

$$\nabla \cdot [D(\mathbf{r}) \nabla G_1(\mathbf{r}, \tau)] - \left[\nu \mu_a(\mathbf{r}) + \frac{1}{3} \nu \mu'_s(\mathbf{r}) k_0^2 \alpha \langle \Delta r^2(\tau) \rangle \right] G_1(\mathbf{r}, \tau) = -\nu S_0 \delta(\mathbf{r}), \quad (1)$$

式中:光子扩散系数 $D(\mathbf{r}) = \nu/3 [\mu'_s(\mathbf{r}) + \mu_a(\mathbf{r})] \approx \nu/3 [\mu'_s(\mathbf{r})]$; 未归一化的电场自相关函数 $G_1(\mathbf{r}, \tau) = \langle \mathbf{E}^*(\mathbf{r}, t) \cdot \mathbf{E}(\mathbf{r}, t + \tau) \rangle^2$; τ 为相关时间或延迟时间; α 取值为 0~1, 为动态散射体占总散射体的比例; $\langle \Delta r^2(\tau) \rangle$ 为时间 τ 内动态散射体的均方位移,对于生物组织而言, $\langle \Delta r^2(\tau) \rangle = 6D_b \tau$, D_b 为有效布朗扩散系数; ∇ 为汉密尔顿算子; ν 为生物组织中的光速; $\mu_a(\mathbf{r})$ 为吸收系数; $\mu'_s(\mathbf{r})$ 为约化散射系数; $S_0 \delta(\mathbf{r})$ 为光源分布。实际测量中,光强往往比电场

强度更易获取,两者满足 Siegert 关系^[21]:

$$g_2(\tau) = 1 + \beta |g_1(\tau)|^2, \quad (2)$$

式中: β 为一常数,通常 $\beta \approx 0.5$; 归一化光强自相关函数 $g_2(\tau) = \langle I(\mathbf{r}, t) I(\mathbf{r}, t + \tau) \rangle / \langle I(\mathbf{r}, t) \rangle^2$, 归一化电场自相关函数 $g_1(\tau) = \langle \mathbf{E}^*(\mathbf{r}, t) \cdot \mathbf{E}(\mathbf{r}, t + \tau) \rangle / \langle |\mathbf{E}(\mathbf{r}, t)| \rangle^2$.

基于 Siegert 关系,可由测量得到的归一化光强自相关函数 $g_2(\tau)$ 推导出归一化电场自相关函数 $g_1(\tau)$,通过非线性最小化算法拟合 $g_1(\tau)$ 与相关扩散方程的解,则可得到用于表征组织血流变化的血流指数 $B_{FI} = \alpha D_b$ 。组织血流与血流指数的关系^[15, 22]满足

$$B_F = \gamma B_{FI}, \quad (3)$$

式中: B_F 为组织血流,单位为 $\text{mL} \cdot 100 \text{ mL}^{-1} \cdot \text{min}^{-1}$; B_{FI} 为血流指数,单位为 $\text{cm}^2 \cdot \text{s}^{-1}$; γ 为校正系数。组织血流变化 (rBF) 和血流指数 B_{FI} 之间满足的关系^[23]为

$$r_{BF} = \frac{B_F}{B_{F0}} - 1 = \frac{\gamma B_{FI}}{\gamma B_{FI0}} - 1 = \frac{B_{FI}}{B_{FI0}} - 1 = r_{BFI}, \quad (4)$$

式中:下标 0 代表初始时刻。可见,获取组织血流变化时无需确定校正系数 γ ,可由血流指数 B_{FI} 的变化得到组织血流变化 r_{BF} 。

2.2 DCS 组织血流检测系统

DCS 组织血流检测系统由光源、探测器、相关

器、光学探头、上位机等部分组成,具有结构简单、操作方便、适用范围广等优势。选取各组成部分时需满足所提及的 Siegert 关系等条件的约束。其中,一般采用 785 nm 波长的激光光源,相关长度应远大于光在被测组织内的传播路径,以确保探测到的散斑波动具有较高对比度,一般大于 5 m,且具有较高的稳定性,功率符合人体辐照安全标准。探测器采用雪崩光电二极管,用于将探测到的光子转化为电脉冲信号,以满足对单光子探测的需求。光学探头由光源光纤和探测光纤组成,光源光纤为多模光纤,探测器光纤为单模光纤。相关器用于计算归一化光强自相关函数 $g_2(\tau)$,可采用商用相关器,以实现大范围延迟时间内的归一化光强自相关函数 $g_2(\tau)$ 计算。

在以上 DCS 组织血流检测系统的基础上,已有研究从时间和空间两个维度分别发展出具有高时间分辨率的快速 DCS 技术^[24-27]和可空间成像的扩散相关断层成像 (DCT) 技术^[28-33]。图 2 展示了基于软件相关器的快速 DCS 所获取的归一化光强自相关函数 $g_2(\tau)$ 和 BFI,相比于传统 DCS 方法,可清晰看到快速 DCS 技术获取的组织血流脉动信息,其组织血流采样率可达 100 Hz^[27, 34]。图 3 展示了用于组织血流三维成像 DCT 系统的光学探头,该光学探头以非接触方式扫描获取被测组织表面的散射光斑波动,可实现乳腺肿瘤与正常乳腺的组织血流的对比成像^[33]。

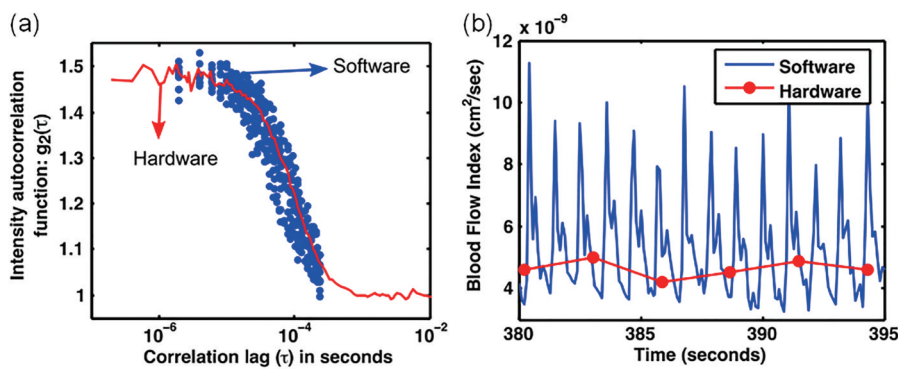


图 2 快速 DCS 与传统 DCS 的组织血流检测对比^[27]。(a) 归一化光强自相关函数; (b) 血流指数

Fig. 2 Comparison between tissue blood flow monitoring using fast DCS and traditional DCS^[27]. (a) Normalized intensity autocorrelation function; (b) blood flow index

进一步的研究^[35]将 DCT 系统应用于两名乳腺癌患者,完整扫描后可实现对乳腺组织血流的三维空间成像。结果显示,两名乳腺癌患者肿瘤区域的平均血流分别是周围健康组织平均血流的 5.9 倍和 10.9 倍。可见, DCT 系统可以在不扭曲组织血流动

力学情况下,对乳腺组织等软组织的血流分布进行成像。此外,在 DCS 与 DOS/DOT 相结合的复合式检测系统方面,已有研究开发了基于 DCS 和时域 DOS/NIRS 的 BabyLux 系统,可实现对新生儿脑组织血流和脑组织氧代谢等参数的检测^[36]。

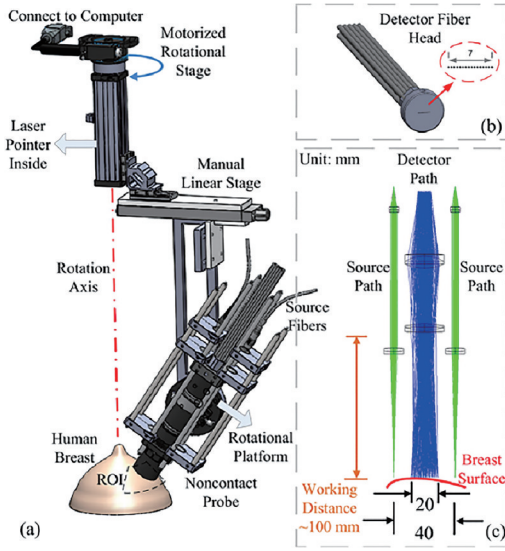


图 3 DCT 系统的非接触式旋转扫描探头^[33]

Fig. 3 Schematic of noncontact DCT system with rotational scanning probe^[33]

2.3 DCS 组织血流检测方法

DCS 将近红外光照射到组织表面,通过探测组织表面散射光斑计算得到归一化光强自相关函数,

拟合出用于表征组织血流变化的血流指数。由 (4) 式可知,血流指数 BFI 的变化可代表组织血流变化 rBF, 即组织血流的相对变化量。为实现对组织血流绝对量的连续检测,已有研究指出血流指数校正算法可完成血流指数 BFI (单位为 $\text{cm} \cdot \text{s}^{-1}$) 与组织血流绝对量 BF (单位为 $\text{mL} \cdot 100 \text{ mL}^{-1} \cdot \text{min}^{-1}$ 或 $\text{mL} \cdot 100 \text{ g}^{-1} \cdot \text{min}^{-1}$) 间的变换,且确定了应用于骨骼肌组织血流和脑组织血流检测的校正系数 γ ,从而实现了骨骼肌血流和脑血流绝对量的连续检测^[23, 37]。图 4 和图 5 分别展示了骨骼肌血流指数和脑血流指数校正算法的实施过程^[23, 37]。

在 BFI 量化方面,传统方法一般通过测量得到的归一化光强自相关函数 $g_2(\tau)$ 以迭代拟合方式实现,已有研究在此基础上提出了 N 阶线性算法等方法^[38-41] 替代传统迭代拟合算法,提高了 $g_2(\tau)$ 量化 BFI 的准确率。

深度学习方法能够从原始数据中直接学习生理信号表征,可替代传统人工特征表示。近年来,基于经典的深度学习框架已实现对生理信号的特

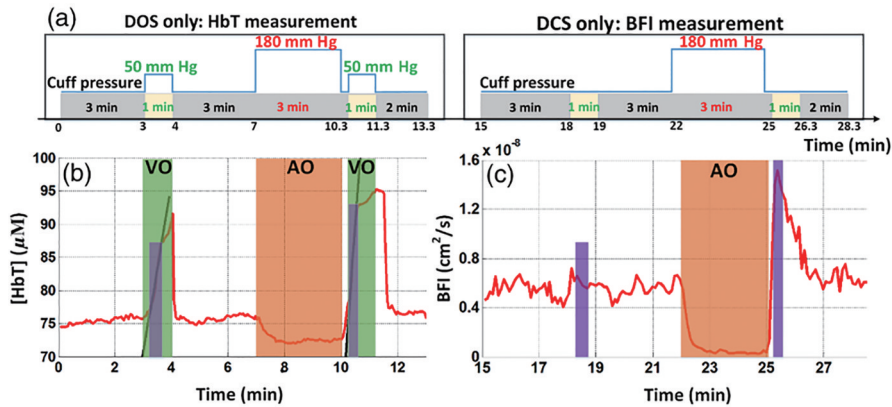


图 4 骨骼肌组织血流指数校正方法^[23]。(a) 测量过程示意图; (b) 总血红蛋白浓度变化; (c) 血流指数变化

Fig. 4 Calibration method of BFI in skeletal muscle^[23]. (a) Experimental protocol; (b) total hemoglobin concentration change; (c) BFI change

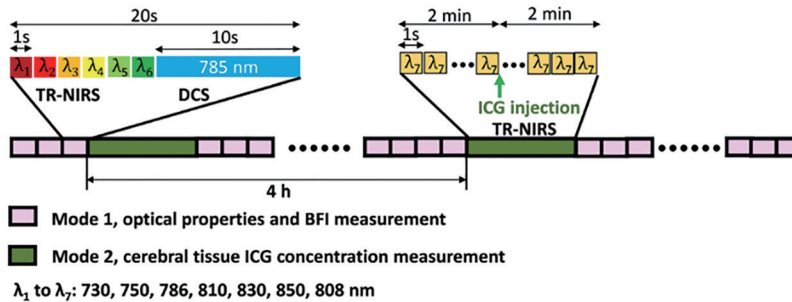


图 5 脑组织血流指数校正方法过程示意图^[37]

Fig. 5 Experimental protocol of the cerebral BFI calibration method^[37]

征提取^[42-43],如利用卷积神经网络实现对散斑图像位移场的测量^[44]。此外,已有研究利用循环神经网络有效抑制了脑功能成像中的心跳、呼吸和低频振荡等生理干扰以及散弹噪声和环境噪声等随机噪声^[45]。鉴于此,将深度学习应用于BFI量化,可以避免传统方法易受到数据噪声影响、计算时间较

长等问题。图 6 展示了基于长短期记忆(LSTM)网络的BFI量化方法,在不降低运算精度的同时,极大地提高了运算速度,与传统拟合算法相比,具有较高的相关性、良好的一致性和较小的差异性,相关系数 r^2 为 0.99,均方根误差(RMSE)为 4.39%,平均绝对误差(MAE)为 3.38%^[46]。

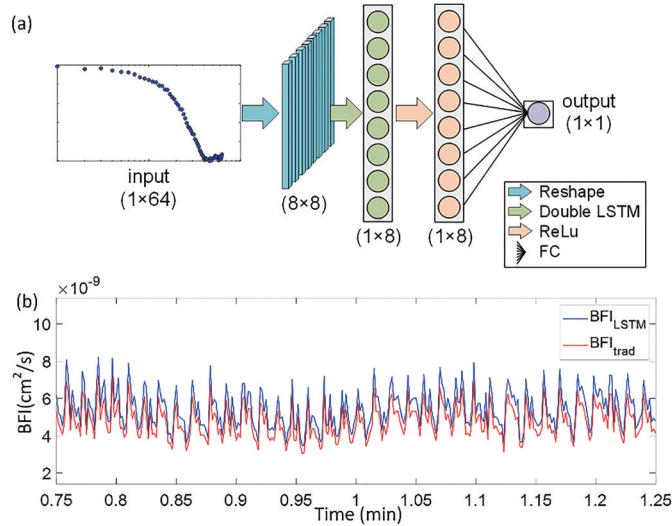


图 6 基于LSTM的BFI量化方法的网络架构^[46]

Fig. 6 Network architecture of the BFI quantification method based on LSTM^[46]

3 扩散相关光谱技术的临床应用

3.1 DCS在脑血流检测中的应用

脑组织中致密的血管网通过血流运输氧气与营养,同时排出代谢产物,缺血性脑卒中(ischemic

stroke)、脑创伤(brain injury)、脑出血(intracerebral hemorrhage)等脑疾病均可引起几天甚至几周的脑自动调节(CA)能力受损,进而造成不可逆的脑损伤。长时间连续实时的脑血流(CBF)检测能够为脑自动调节监测提供有力保障,如图 7 所示,DCS 能够

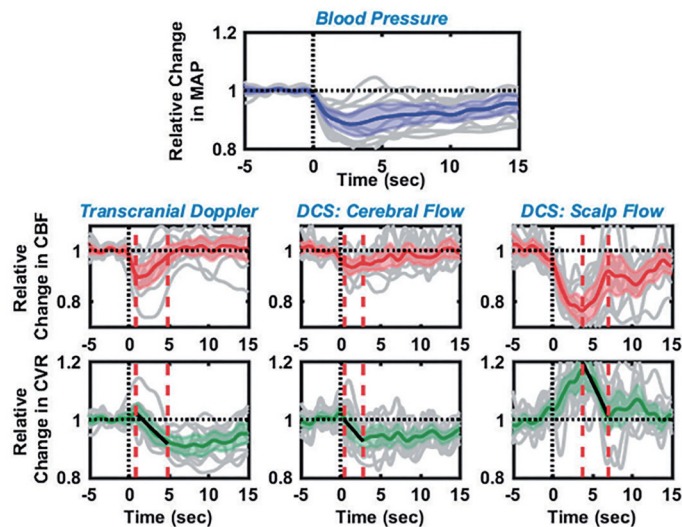


图 7 脑自动调节评估中 11 名健康人的脑血流(CBF)和脑血管阻力(CVR)变化^[47]

Fig. 7 Changes of cerebral blood flow (CBF) and cerebrovascular resistance (CVR) in 11 healthy subjects during cerebral autoregulation evaluation^[47]

在健康人的脑自动调节评估试验中可直接检测颅内血流和颅外血流的实时变化,并同时提供脑血管阻力实时变化^[47]。进一步研究表明,DCS可监测受损脑自动调节[如图8(a)所示]和完整脑自动调节[如图8(b)所示]过程中脑血流的实时变化,与平均动脉压(MAP)和颅内压(ICP)等参数对比,为临床上脑自动调节能力的即时诊断提供判断依据^[48]。

机械性血栓清除术(mechanical thrombectomy)

是治疗大血管阻塞所致急性脑卒中的重要方法。图9(a)展示了机械性血栓清除术前及术后一名患者的脑血流CT图像^[49],现有的脑梗死评分无法描述微血管灌注问题,因此无法得知大血管再通后脑组织血流动力学效果。如图9(b)、(c)所示,DCS可实时提供颈内动脉(ICA)堵塞和再通后同侧及对侧脑血流的变化,为机械性血栓清除术的术后微血管测量提供有利参考^[49]。

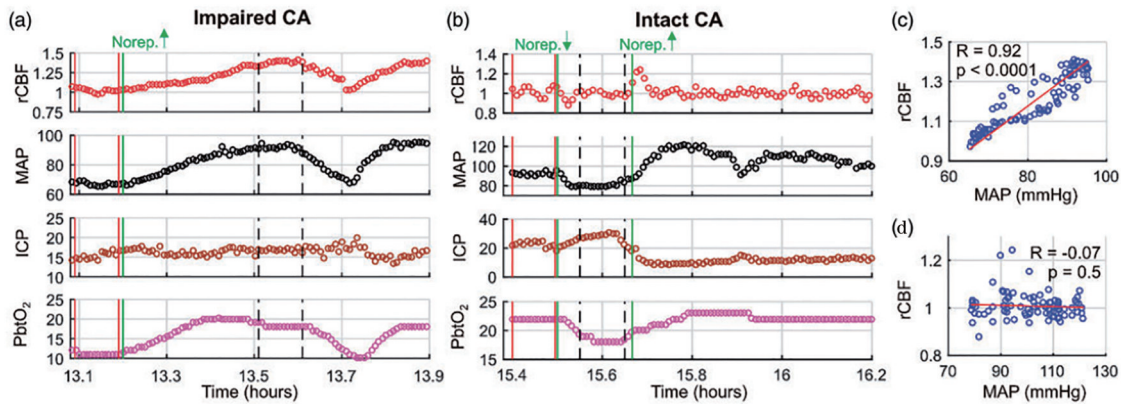


图 8 受损脑自动调节和完整脑自动调节过程中脑血流、平均动脉压、颅内压、脑氧张力的变化^[48]

Fig. 8 Changes of cerebral blood flow, mean arterial pressure, intracranial pressure, and cerebral oxygen tension during impaired cerebral autoregulation and intact cerebral autoregulation^[48]

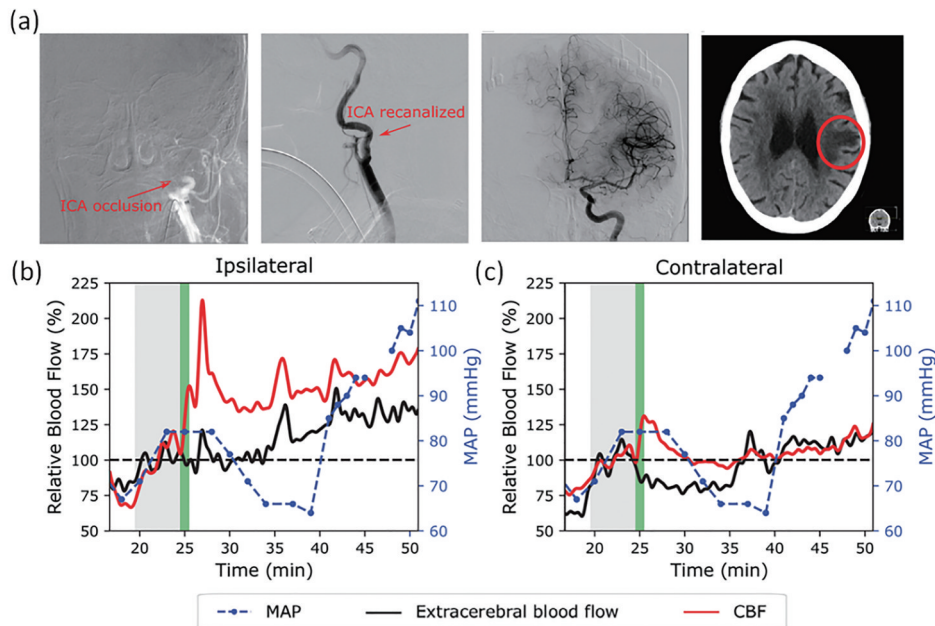


图 9 机械性血栓清除术前和术后的脑血流图像及颈内动脉再通前后同侧及对侧脑血流变化^[49]

Fig. 9 Cerebral blood flow images before and after mechanical thrombectomy and cerebral blood flow monitoring before, during, and after internal carotid artery recanalization^[49]

此外,胸内压(intrathoracic pressure)直接影响心脏的出血量,亦可引起脑血流的变化。图10为不同胸内压(6 cmH₂O和12 cmH₂O)条件下DCS实时

检测的脑血流变化,并将其与TCD所检测的脑中动脉血流变化进行对比^[50],从图中可清晰地看出脑血流脉动变化。

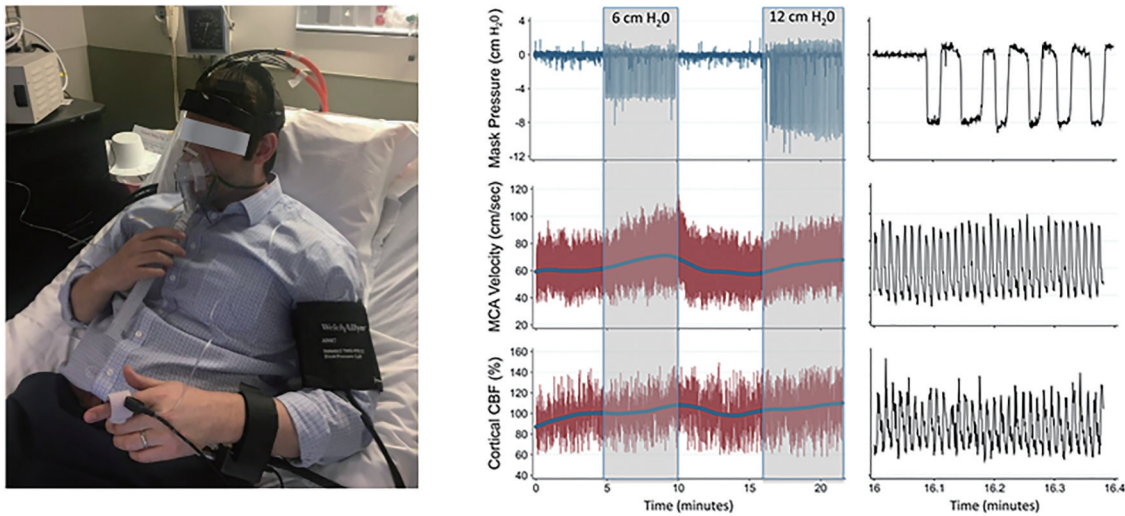


图 10 胸内压变化情况下的脑血流时序图^[50]

Fig. 10 Time series diagrams of cerebral blood flow under the change of intrathoracic pressure^[50]

3.2 DCS在骨骼肌血流检测中的应用

对血管类疾病(如外周动脉疾病、纤维肌痛等)的诊疗依赖于相应部位的骨骼肌血流循环状态,脂肪沉积、粥样形成等引起的血管阻塞或硬化影响着组织血流传输和组织氧代谢,严重影响

患者日常生活。因此,对骨骼肌组织血流变化的检测至关重要。图 11 展示了 DCS 光学探头放置于小腿腓肠肌部位时的 MRI 图像和在大腿根部袖带加压过程中小腿腓肠肌组织血流的变化^[17]。

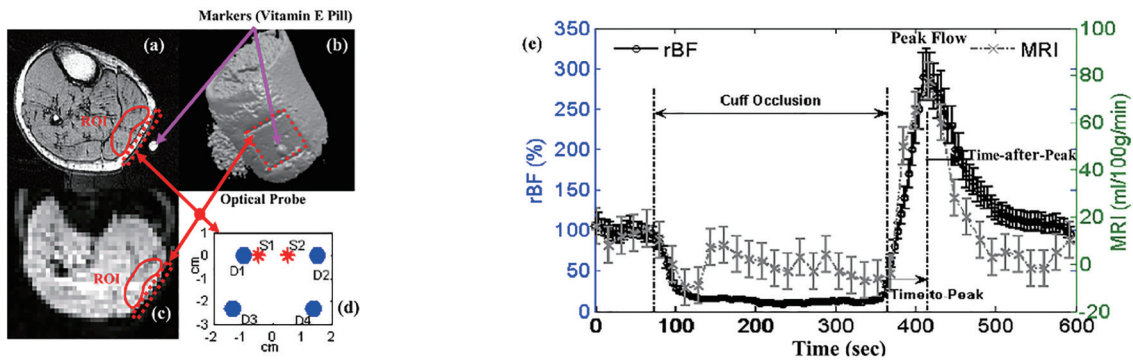


图 11 DCS 光学探头放置于腓肠肌处的组织血流变化^[17]。(a)~(c)腓肠肌 MRI 图像;(d) DCS 光学探头距离示意图;(e)袖带加压过程中腓肠肌组织血流变化

Fig. 11 Blood flow changes of gastrocnemius muscle tissue obtained by DCS optical probe^[17]. (a) - (c) MRI images of gastrocnemius muscle; (d) diagram of DCS optical probe distance; (e) changes of blood flow in gastrocnemius muscle during cuff compression

外周动脉疾病是最常见的血管类疾病之一,间歇性跛行是其临床特性表现,严重可导致截肢。介入治疗多采用旁路移植术(ABG)或者经皮腔内血管成形术(PTA),但术后血管再狭窄发生率高(约 30%),且没有对肌肉血管重建效果评估的标准。DCS 可以检测在血管重建手术过程中小腿腓肠肌部位的组织血流变化^[51],如图 12 所示,可以看出:在夹持股动脉期间,腓肠肌组织血流明显下降;松开动脉夹后,腓肠肌出现明显的反应性充血,即组织血流显著上升;术后

腓肠肌组织血流高于术前基线组织血流。

除介入手术治疗方法外,外周动脉疾病患者还可进行腿部或者手臂运动训练以缓解病痛。因此,对其评估通常以动态方式进行,如平卧双脚摆动试验、直立抬足跟试验、平板运动负荷试验等。而临床上,运动训练对缓解外周动脉疾病患者病痛的机理尚不清楚,DCS 获取了外周动脉疾病患者进行三个月平板运动负荷试验前后的组织血流变化^[52],如图 13 所示,运动组外周动脉疾病患者的组织血流变

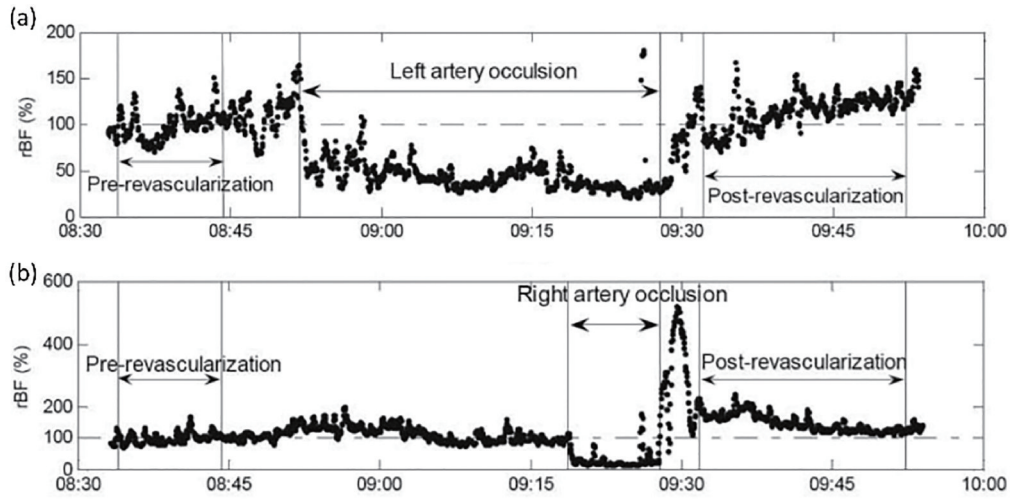


图 12 一位外周动脉疾病患者在双股动脉旁路移植术中的肌肉组织血流变化^[51]。(a)左腿腓肠肌组织血流变化；(b)右腿腓肠肌组织血流变化

Fig. 12 Typical muscle hemodynamic responses during bi-femoral artery bypass graft in a patient with peripheral arterial disease (PAD)^[51]. (a) rBF in left calf muscle; (b) rBF in right calf muscle

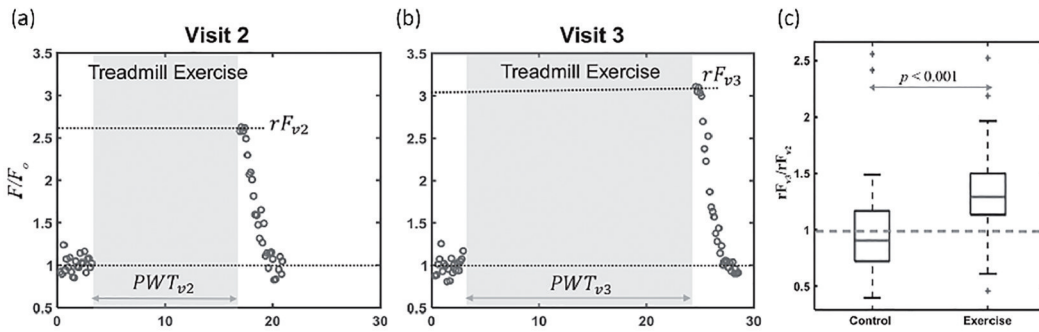


图 13 三个月前后外周动脉疾病患者对比结果^[52]。(a)三个月前的组织血流变化；(b)三个月后平板运动负荷试验下的组织血流变化；(c)运动组与对照组三个月前后组织血流变化箱型图

Fig. 13 Comparison results in a PAD patient before and after 3-month exercise training^[52]. (a) Changes of tissue blood flow three months ago; (b) changes of tissue blood flow under treadmill exercise load test after three months; (c) box diagram of tissue blood flow changes in exercise group and control group before and after three months

化明显高于对照组的组织血流变化。进一步研究表明^[53],运动训练能够提高静息状态下腓肠肌的氧代谢水平,原因在于运动训练增强了腓肠肌静息状态下组织氧摄取能力,如图 14 所示。

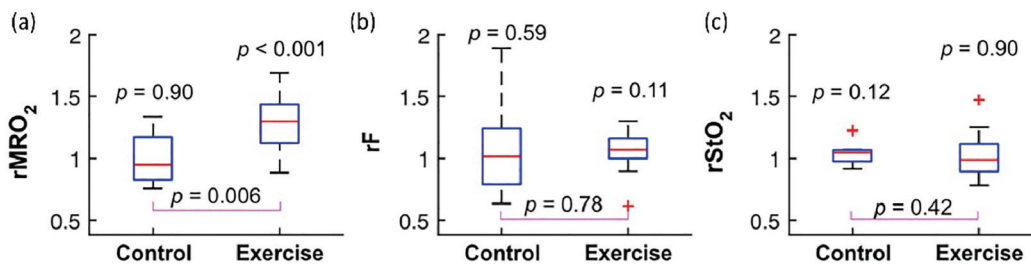


图 14 三个月前后运动组和对照组外周动脉疾病患者腓肠肌参数变化^[53]。(a)氧代谢率变化；(b)组织血流变化；(c)组织氧饱和度变化

Fig. 14 Changes of gastrocnemius parameters in exercise group and control group of a PAD patient before and after three months^[53]. (a) Metabolic rate of oxygen (rMRO₂); (b) relative blood flow (rF); (c) tissue oxygen saturation (rStO₂)

此外,鉴于动态方式评估对临床诊断的重要性,DCS亦可实现骑行过程中对组织血流变化的检测^[54],被测试者以 80~100 r/min 的速度骑行直至疲

劳为止,如图 15 所示,可检测到组织血流随骑行功率的增加而增加。可见,DCS 骨骼肌血流检测能够为外周动脉疾病等的诊断和机理探寻提供有力支持。

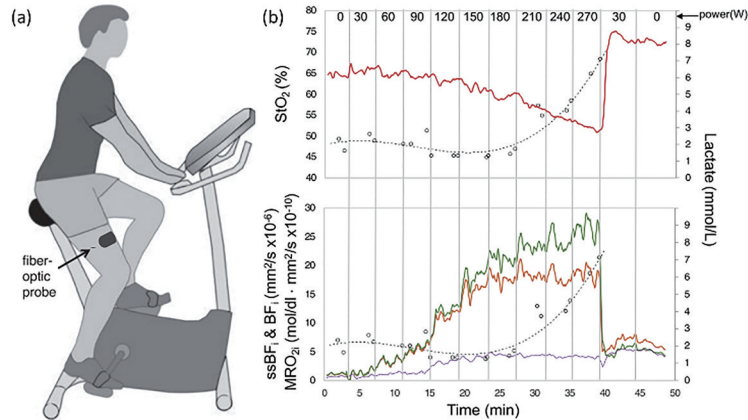


图 15 骑行运动中组织血流和组织氧饱和度的变化^[54]。(a)骑行运动示意图;(b)一名被测试者在骑行运动中的组织血流指数和组织氧饱和度变化

Fig. 15 Changes of muscle BFI and StO₂ during the cycling exercise^[54]. (a) Schematic of riding; (b) muscle BFI and StO₂ for a representative subject during the cycling exercise

3.3 DCS在肿瘤血流检测中的应用

早期癌症检测可以显著提高治疗效果,而在目前癌症的临床常规诊疗中缺乏对肿瘤的血液动力学

和代谢水平的监测。图 16 和图 17 分别展示了 DCS 技术应用于头颈癌^[55-56]和乳腺癌^[57]的组织血流检测。图 16(b)为对头颈癌肿瘤进行放射治疗后的组织血

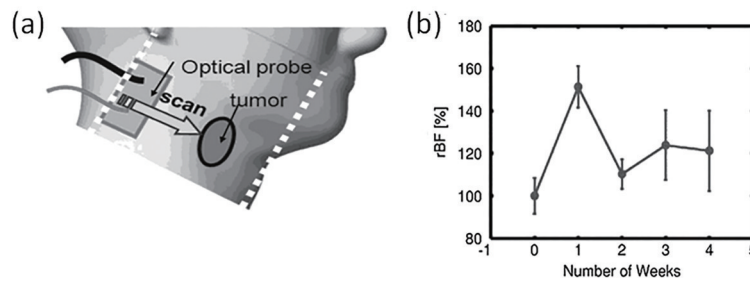


图 16 头颈癌组织血流检测^[55-56]。(a)手持式检测探头位置示意图;(b)头颈癌患者在放射治疗后的肿瘤平均组织血流变化

Fig. 16 Tissue blood flow monitoring of neck/head tumor^[55-56]. (a) Position diagram of hand-held detection probe; (b) average tumor rBF changes in patients with head and neck cancer after radiotherapy

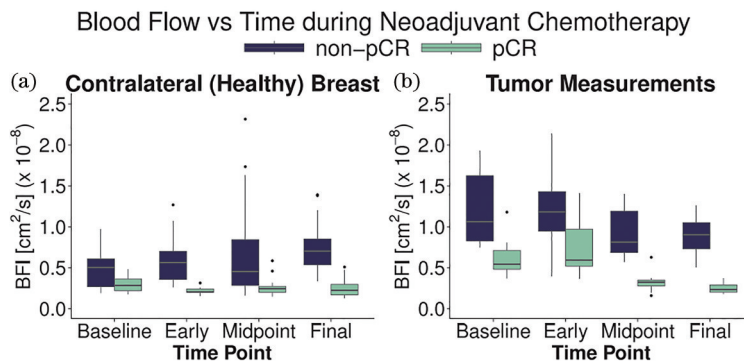


图 17 新辅助化疗过程中乳腺组织血流指数变化箱型图^[57]。(a)健康乳腺;(b)肿瘤乳腺

Fig. 17 Box diagrams of breast tissue blood flow index changes during the neoadjuvant chemotherapy (NAC) treatment^[57]. (a) Healthy breast; (b) tumor breast

流变化,图 17(a)为健康乳腺在新辅助化疗下不同时间点的血流指数变化,图 17(b)为肿瘤乳腺在新辅助化疗下不同时间点的血流指数变化。可以看出,对于肿瘤组织血流等参数的检测,DCS 能够为头颈癌^[58-60]和乳腺癌^[61-62]等癌症早期诊断提供依据。

4 扩散相关光谱技术的展望

DCS 技术的穿透深度虽然远大于激光散斑成像(LSCI)技术,但与其他近红外光学技术类似,与传统的临床血流检测技术(如 MRI 和 CT)相比仍存在不足。MRI 和 CT 的检测范围可覆盖全脑,但 DCS 由于穿透深度一般为光源-探测器间距的一半,通常 DCS 光源-探测器间距为 2~4 cm,DCS 无法获取更为深层(大于 2 cm)的脑血流变化。为提高 DCS 的穿透深度,已有研究致力于提高大间距下 DCS 信号获取的信噪比,如改进探测器件^[63]或利用少模光纤^[64]等。此外,DCS 血流检测通过探测组织表面散射光斑变化推算组织中红细胞的运动状态,因此光学探头与被测组织间的位移偏差会为 BFI 的拟合引入噪声,从而导致 DCS 血流检测对运动变化

较为敏感。为解决此问题,DCS 可采用与 DOS/NIR 类似的分析方法(如主成分分析、小波分析、样条插值等)减小光学探头移动引起的误差,亦可探究快速 DCS 是否适用于对运动中组织血流的检测。

相比于其他血流检测技术,DCS 克服了激光多普勒、核磁共振等临床血流检测技术存在的辐射、实时性连续性差、操作难度大等问题。表 1 对比了 DCS 与多种组织血流检测技术^[65],从中可以看出 DCS 具有适用年龄范围大、无创、不需要造影剂、无辐射危害、能床边检测、采集时间短及仪器成本低等优势。从临床角度而言,DCS 血流检测设备具备安全、无创、低成本、便携等特点,因此 DCS 可作为重症监护病房和手术室中的床边脑灌注监测仪。相比于 DOS/NIRS 组织氧检测,DCS 能够提供微血管的血流量信息,因此可为组织氧输送提供有价值的补充信息,为临床医生提供比单一组织氧或组织血流等更全面的生理评估参数。未来,DCS 有望在脑疾病、骨骼肌疾病和癌症等的实时监测和早期诊断方面早日步入临床,为心脑血管类疾病和癌症等的诊疗提供新技术。

表 1 组织血流检测方法对比^[65]

Table 1 Comparison of tissue blood flow monitoring methods^[65]

Item	PET	SPECT	XeCT	CT-P	DSC-MRI	ASL-MRI	DU	DCS
Age range	A, C	A, C	A, C	A, C	A, C	A, C, N	A, C, N	A, C, N
Bedside	No	Sometimes	No	No	No	No	Yes	Yes
Contrast agent	Yes	Yes	Yes	Yes	Yes	No	No	No
Radiation	Yes	Yes	Yes	Yes	No	No	No	No
Acquisition time	5-9 min	10-15 min	10 min	40 s	1 min	5-10 min	1-20 min	0.5-6 s
Parameters	CBF	CBF	CBF	MTT	MTT	CBF	BFV	CBF
Large vessel	Ok	Ok	Ok	Problem	Problem	Ok	ONLY	Microvascular
Quantitative	Yes	Sometimes	Yes	Yes	N/A	Yes	N/A	Relative
Brain coverage	Whole	Whole	6 cm thick	5 cm thick	Whole	Whole	~3/hemisphere	~Few/hemisphere
Spatial resolution	~5 mm	~5 mm	~5 mm	~1.5 mm	~2 mm	~2 mm	N/A	~10 mm
Intrascan time	10 min	10 min	20 min	10 min	25 min	0 min	0 min	0 min
Emergency setting	No	Sometimes	Yes	Yes	Yes	Yes	Yes	Yes
Instrument cost	High	High	Moderate	Moderate	High	High	Low	Low

注释:PET 指正电子发射断层成像技术,SPECT 指单光子发射计算机断层成像术,XeCT 指氙增强计算机断层扫描技术,CT-P 代表 CT 灌注成像技术,DCS-MRI 指动态增强核磁共振技术,ASL-MRI 指动态自旋标记核磁共振技术,DU 指多普勒超声。

5 结束语

DCS 技术是一项组织血流无创检测技术,能够实现深层组织血流的连续、实时、长时间的检测,且已得到了核磁共振、激光多普勒等多种临床血流检测技术的验证。该技术将近红外光照射到被测

组织表面,通过推算红细胞的运动状态实现组织血流变化检测,测量过程中被测试者无任何不适,满足昼夜床边检测要求,且可追踪突发异常时血流变化。DCS 检测系统结构简单、成本低、光纤耦合探头与被测试者接触面积小、检测要求低、操作方便,适用于新生儿、孕妇、重症人群等。新发展的快速

DCS 和 DCT 能够为穿透深度和运动敏感等问题的解决提供新方法,进一步拓展了 DCS 的应用范围。随着科学技术的不断发展,DCS 有望广泛应用于对脑血流、骨骼肌血流和肿瘤血流的无创检测,在脑血管类疾病和癌症等的诊疗方面将展现出巨大的临床应用价值。

参 考 文 献

- [1] Wang L D, Liu J M, Yang Y, et al. The prevention and treatment of stroke still face huge challenges: brief report on stroke prevention and treatment in China, 2018[J]. Chinese Circulation Journal, 2019, 34(2): 105-119.
王陇德, 刘建民, 杨弋, 等. 我国脑卒中防治仍面临巨大挑战:《中国脑卒中防治报告 2018》概要[J]. 中国循环杂志, 2019, 34(2): 105-119.
- [2] Ye G W, Zhong G L, Chen X G, et al. Effect of different input arteries on CT perfusion imaging parameters of brain in patients with internal carotid artery stenosis[J]. Chinese Journal of Medical Imaging, 2018, 26(10): 742-746.
叶国伟, 钟根龙, 陈旭高, 等. 不同输入动脉对颈内动脉狭窄患者颅脑 CT 灌注成像参数的影响[J]. 中国医学影像学杂志, 2018, 26(10): 742-746.
- [3] Wang C F, Wang B J, Wang Z, et al. Application of multi-modal MRI and fusion technique on the radiotherapy dose optimization of postoperative glioma [J]. Chinese Journal of Practical Nervous Diseases, 2019, 22(11): 1179-1185.
王长福, 王斌杰, 王智, 等. 磁共振多模态成像及融合技术在脑胶质瘤术后放疗剂量优化中的应用[J]. 中国实用神经疾病杂志, 2019, 22(11): 1179-1185.
- [4] Liu M, Li X D. Application progress of magnetic resonance imaging in acute ischemic stroke[J]. Medical Recapitulate, 2019, 25(3): 576-582.
刘敏, 李晓东. 急性缺血性脑卒中的影像学应用进展[J]. 医学综述, 2019, 25(3): 576-582.
- [5] Ning L, Sun H, Feng J, et al. Research progress in prevention and treatment strategy of acute ischemic stroke[J]. Medical Recapitulate, 2022, 28(1): 94-99.
宁珑, 孙航, 冯晋, 等. 急性缺血性脑卒中防治策略研究进展[J]. 医学综述, 2022, 28(1): 94-99.
- [6] Fan A P, Khalil A A, Fiebach J B, et al. Elevated brain oxygen extraction fraction measured by MRI susceptibility relates to perfusion status in acute ischemic stroke[J]. Journal of Cerebral Blood Flow and Metabolism: Official Journal of the International Society of Cerebral Blood Flow and Metabolism, 2020, 40(3): 539-551.
- [7] Oddo M, Villa F, Citerio G. Brain multimodality monitoring: an update[J]. Current Opinion in Critical Care, 2012, 18(2): 111-118.
- [8] Le R P. Physiological monitoring of the severe traumatic brain injury patient in the intensive care unit [J]. Current Neurology and Neuroscience Reports, 2013, 13(3): 331.
- [9] Sandsmark D K, Kumar M A, Park S, et al. Multimodal monitoring in subarachnoid hemorrhage [J]. Stroke, 2012, 43(5): 1440-1445.
- [10] Boas D A, Yodh A G. Spatially varying dynamical properties of turbid media probed with diffusing temporal light correlation[J]. Journal of the Optical Society of America A, 1997, 14(1): 192-215.
- [11] Boas D A, Campbell L E, Yodh A G. Scattering and imaging with diffusing temporal field correlations [J]. Physical Review Letters, 1995, 75(9): 1855-1858.
- [12] Durduran T, Choe R, Baker W B, et al. Diffuse optics for tissue monitoring and tomography[J]. Reports on Progress in Physics, 2010, 73(7): 076701.
- [13] Yodh A, Chance B. Spectroscopy and imaging with diffusing light[J]. Physics Today, 1995, 48(3): 34-40.
- [14] Yu G Q, Durduran T, Zhou C, et al. Noninvasive monitoring of murine tumor blood flow during and after photodynamic therapy provides early assessment of therapeutic efficacy[J]. Clinical Cancer Research: an Official Journal of the American Association for Cancer Research, 2005, 11(9): 3543-3552.
- [15] Buckley E M, Cook N M, Durduran T, et al. Cerebral hemodynamics in preterm infants during positional intervention measured with diffuse correlation spectroscopy and transcranial Doppler ultrasound[J]. Optics Express, 2009, 17(15): 12571-12581.
- [16] Durduran T, Zhou C, Buckley E M, et al. Optical measurement of cerebral hemodynamics and oxygen metabolism in neonates with congenital heart defects [J]. Journal of Biomedical Optics, 2010, 15(3): 037004.
- [17] Yu G Q, Floyd T F, Durduran T, et al. Validation of diffuse correlation spectroscopy for muscle blood flow with concurrent arterial spin labeled perfusion MRI[J]. Optics Express, 2007, 15(3): 1064-1075.
- [18] Kim M N, Durduran T, Frangos S, et al. Noninvasive measurement of cerebral blood flow and blood oxygenation using near-infrared and diffuse

- correlation spectroscopies in critically brain-injured adults[J]. *Neurocritical Care*, 2010, 12(2): 173-180.
- [19] Liu Y, Liu D Y, Zhang Y, et al. A portable fNIRS-topography system for BCI applications: full parallel detection and pilot paradigm validation[J]. *Chinese Journal of Lasers*, 2021, 48(11): 1107001.
刘洋, 刘东远, 张耀, 等. 面向脑机接口应用的便携式 fNIRS 拓扑成像系统: 全并行检测与初步范式实验[J]. *中国激光*, 2021, 48(11): 1107001.
- [20] Mohammad P P S, Isarangura S, Eddins A, et al. Comparison of functional activation responses from the auditory cortex derived using multi-distance frequency domain and continuous wave near-infrared spectroscopy[J]. *Neurophotonics*, 2021, 8(4): 045004.
- [21] Lemieux P A, Durian D J. Investigating non-Gaussian scattering processes by using N th-order intensity correlation functions[J]. *Journal of the Optical Society of America A*, 1999, 16(7): 1651-1664.
- [22] Carp S A, Dai G P, Boas D A, et al. Validation of diffuse correlation spectroscopy measurements of rodent cerebral blood flow with simultaneous arterial spin labeling MRI; towards MRI-optical continuous cerebral metabolic monitoring[J]. *Biomedical Optics Express*, 2010, 1(2): 553-565.
- [23] Li Z, Baker W B, Parthasarathy A B, et al. Calibration of diffuse correlation spectroscopy blood flow index with venous-occlusion diffuse optical spectroscopy in skeletal muscle[J]. *Journal of Biomedical Optics*, 2015, 20(12): 125005.
- [24] Li J, Jaillon F, Dietsche G, et al. Pulsation-resolved deep tissue dynamics measured with diffusing-wave spectroscopy[J]. *Optics Express*, 2006, 14(17): 7841-7851.
- [25] Dietsche G, Ninck M, Ortolfo C, et al. Fiber-based multispeckle detection for time-resolved diffusing-wave spectroscopy: characterization and application to blood flow detection in deep tissue[J]. *Applied Optics*, 2007, 46(35): 8506-8514.
- [26] Dong J, Bi R Z, Ho J H, et al. Diffuse correlation spectroscopy with a fast Fourier transform-based software autocorrelator[J]. *Journal of Biomedical Optics*, 2012, 17(9): 097004.
- [27] Wang D T, Parthasarathy A B, Baker W B, et al. Fast blood flow monitoring in deep tissues with real-time software correlators[J]. *Biomedical Optics Express*, 2016, 7(3): 776-797.
- [28] Huang C, Irwin D, Lin Y, et al. Speckle contrast diffuse correlation tomography of complex turbid medium flow[J]. *Medical Physics*, 2015, 42(7): 4000-4006.
- [29] Huang C, Irwin D, Zhao M J, et al. Noncontact 3-D speckle contrast diffuse correlation tomography of tissue blood flow distribution[J]. *IEEE Transactions on Medical Imaging*, 2017, 36(10): 2068-2076.
- [30] Lin Y, Huang C, Irwin D, et al. Three-dimensional flow contrast imaging of deep tissue using noncontact diffuse correlation tomography[J]. *Applied Physics Letters*, 2014, 104(12): 121103.
- [31] Mazdeyasna S, Huang C, Zhao M J, et al. Noncontact speckle contrast diffuse correlation tomography of blood flow distributions in tissues with arbitrary geometries[J]. *Journal of Biomedical Optics*, 2018, 23(9): 096005.
- [32] Zhao M J, Mazdeyasna S, Huang C, et al. Noncontact speckle contrast diffuse correlation tomography of blood flow distributions in burn wounds: a preliminary study [J]. *Military Medicine*, 2019, 185(S1): 82-87.
- [33] Huang C, Lin Y, He L, et al. Alignment of sources and detectors on breast surface for noncontact diffuse correlation tomography of breast tumors[J]. *Applied Optics*, 2015, 54(29): 8808-8816.
- [34] Yu G Q. Diffuse correlation spectroscopy (DCS): a diagnostic tool for assessing tissue blood flow in vascular-related diseases and therapies[J]. *Current Medical Imaging Reviews*, 2012, 8(3): 194-210.
- [35] He L, Lin Y, Huang C, et al. Noncontact diffuse correlation tomography of human breast tumor[J]. *Journal of Biomedical Optics*, 2015, 20(8): 086003.
- [36] Giovannella M, Contini D, Pagliazzi M, et al. BabyLux device: a diffuse optical system integrating diffuse correlation spectroscopy and time-resolved near-infrared spectroscopy for the neuromonitoring of the premature newborn brain[J]. *Neurophotonics*, 2019, 6(2): 025007.
- [37] He L, Baker W B, Milej D, et al. Noninvasive continuous optical monitoring of absolute cerebral blood flow in critically ill adults[J]. *Neurophotonics*, 2018, 5(4): 045006.
- [38] Shang Y, Yu G Q. A N th-order linear algorithm for extracting diffuse correlation spectroscopy blood flow indices in heterogeneous tissues[J]. *Applied Physics Letters*, 2014, 105(13): 133702.
- [39] Shang Y, Li T, Chen L, et al. Extraction of diffuse correlation spectroscopy flow index by integration of N th-order linear model with Monte Carlo simulation [J]. *Applied Physics Letters*, 2014, 104(19): 193703.
- [40] Zhang P, Gui Z G, Guo G D, et al. Approaches to

- denoise the diffuse optical signals for tissue blood flow measurement[J]. *Biomedical Optics Express*, 2018, 9(12): 6170-6185.
- [41] Zhang X J, Gui Z G, Qiao Z W, et al. Nth-order linear algorithm for diffuse correlation tomography[J]. *Biomedical Optics Express*, 2018, 9(5): 2365-2382.
- [42] Bi X J, Qiao W Z. Learning robust features from EEG based on improved deep-learning model C-NTM[J]. *Journal of Harbin Engineering University*, 2019, 40(9): 1642-1649.
毕晓君, 乔伟征. 基于改进深度学习模型 C-NTM 的脑电鲁棒特征学习[J]. *哈尔滨工程大学学报*, 2019, 40(9): 1642-1649.
- [43] Baloglu U B, Talo M, Yildirim O, et al. Classification of myocardial infarction with multi-lead ECG signals and deep CNN[J]. *Pattern Recognition Letters*, 2019, 122: 23-30.
- [44] Huang J, Sun C R, Lin X L. Displacement field measurement of speckle images using convolutional neural network[J]. *Acta Optica Sinica*, 2021, 41(20): 2012002.
黄举, 孙翠茹, 林祥龙. 基于卷积神经网络的散斑图像位移场测量方法[J]. *光学学报*, 2021, 41(20): 2012002.
- [45] Liu D Y, Zhang Y, Liu Y, et al. LSTM-based recurrent neural network for noise suppression in fNIRS neuroimaging: network design and pilot validation[J]. *Chinese Journal of Lasers*, 2021, 48(19): 1918007.
刘东远, 张耀, 刘洋, 等. 基于 LSTM 循环神经网络的 fNIRS 脑功能成像滤波方法[J]. *中国激光*, 2021, 48(19): 1918007.
- [46] Li Z, Ge Q S, Feng J C, et al. Quantification of blood flow index in diffuse correlation spectroscopy using long short-term memory architecture[J]. *Biomedical Optics Express*, 2021, 12(7): 4131-4146.
- [47] Parthasarathy A B, Gannon K P, Baker W B, et al. Dynamic autoregulation of cerebral blood flow measured non-invasively with fast diffuse correlation spectroscopy[J]. *Journal of Cerebral Blood Flow and Metabolism: Official Journal of the International Society of Cerebral Blood Flow and Metabolism*, 2018, 38(2): 230-240.
- [48] Baker W B, Balu R, He L, et al. Continuous noninvasive optical monitoring of cerebral blood flow and oxidative metabolism after acute brain injury[J]. *Journal of Cerebral Blood Flow and Metabolism*, 2019, 39(8): 1469-1485.
- [49] Forti R M, Favilla C G, Cochran J M, et al. Transcranial optical monitoring of cerebral hemodynamics in acute stroke patients during mechanical thrombectomy [J]. *Journal of Stroke and Cerebrovascular Diseases*, 2019, 28(6): 1483-1494.
- [50] Favilla C G, Forti R M, Zamzam A, et al. Perfusion enhancement with respiratory impedance after stroke (PERI-stroke) [J]. *Neurotherapeutics*, 2019, 16(4): 1296-1303.
- [51] Yu G Q, Shang Y, Zhao Y Q, et al. Intraoperative evaluation of revascularization effect on ischemic muscle hemodynamics using near-infrared diffuse optical spectroscopies[J]. *Journal of Biomedical Optics*, 2011, 16(2): 027004.
- [52] Baker W B, Li Z, Schenkel S S, et al. Effects of exercise training on calf muscle oxygen extraction and blood flow in patients with peripheral artery disease[J]. *Journal of Applied Physiology*, 2017, 123(6): 1599-1609.
- [53] Li Z, Englund E K, Langham M C, et al. Exercise training increases resting calf muscle oxygen metabolism in patients with peripheral artery disease[J]. *Metabolites*, 2021, 11(12): 814.
- [54] Quaresima V, Farzam P, Anderson P, et al. Diffuse correlation spectroscopy and frequency-domain near-infrared spectroscopy for measuring microvascular blood flow in dynamically exercising human muscles [J]. *Journal of Applied Physiology*, 2019, 127(5): 1328-1337.
- [55] Yu G Q. Near-infrared diffuse correlation spectroscopy in cancer diagnosis and therapy monitoring[J]. *Journal of Biomedical Optics*, 2012, 17(1): 010901.
- [56] Sunar U, Quon H, Durduran T, et al. Noninvasive diffuse optical measurement of blood flow and blood oxygenation for monitoring radiation therapy in patients with head and neck tumors: a pilot study[J]. *Journal of Biomedical Optics*, 2006, 11(6): 064021.
- [57] Cochran J M, Chung S H, Leproux A, et al. Longitudinal optical monitoring of blood flow in breast tumors during neoadjuvant chemotherapy[J]. *Physics in Medicine and Biology*, 2017, 62(12): 4637-4653.
- [58] Irwin D, Dong L X, Shang Y, et al. Influences of tissue absorption and scattering on diffuse correlation spectroscopy blood flow measurements[J]. *Biomedical Optics Express*, 2011, 2(7): 1969-1985.
- [59] Dong L, Kudrimoti M, Cheng R, et al. Noninvasive diffuse optical monitoring of head and neck tumor blood flow and oxygenation during radiation delivery [J]. *Biomedical Optics Express*, 2012, 3(2): 259-272.

- [60] Dong L X, Kudrimoti M, Irwin D, et al. Diffuse optical measurements of head and neck tumor hemodynamics for early prediction of chemoradiation therapy outcomes[J]. *Journal of Biomedical Optics*, 2016, 21(8): 085004.
- [61] Cochran J M, Busch D R, Leproux A, et al. Tissue oxygen saturation predicts response to breast cancer neoadjuvant chemotherapy within 10 days of treatment [J]. *Journal of Biomedical Optics*, 2018, 24(2): 021202.
- [62] Agochukwu N B, Huang C, Zhao M J, et al. A novel noncontact diffuse correlation spectroscopy device for assessing blood flow in mastectomy skin flaps: a prospective study in patients undergoing prosthesis-based reconstruction[J]. *Plastic and Reconstructive Surgery*, 2017, 140(1): 26-31.
- [63] Cortese L, Lo Presti G, Pagliuzzi M, et al. Recipes for diffuse correlation spectroscopy instrument design using commonly utilized hardware based on targets for signal-to-noise ratio and precision[J]. *Biomedical Optics Express*, 2021, 12(6): 3265-3281.
- [64] He L, Lin Y, Shang Y, et al. Using optical fibers with different modes to improve the signal-to-noise ratio of diffuse correlation spectroscopy flow-oximeter measurements[J]. *Journal of Biomedical Optics*, 2013, 18(3): 037001.
- [65] Durduran T, Yodh A G. Diffuse correlation spectroscopy for noninvasive, micro-vascular cerebral blood flow measurement[J]. *NeuroImage*, 2014, 85: 51-63.